We are IntechOpen,
the world's leading publisher of
Open Access books
Built by scientists, for scientists

6,900
Open access books available

186,000
International authors and editors

200M
Downloads

154
Countries delivered to

Our authors are among the

TOP 1%
most cited scientists

12.2%
Contributors from top 500 universities

Interested in publishing with us?
Contact book.department@intechopen.com

Numbers displayed above are based on latest data collected.
For more information visit www.intechopen.com

Comparative Analysis of Three Digital Signal Processing Techniques for 2D Combination of Echographic Traces Obtained from Ultrasonic Transducers Located at Perpendicular Planes

Miguel A. Rodríguez-Hernández[1], Antonio Ramos[2] and J. L. San Emeterio[2]
[1]ITACA. Universitat Politècnica de Valencia
[2]Lab. Ultrasonic Signal, Systems and Technologies, CSIC. Madrid
Spain

1. Introduction

In certain practical cases of quality control in the manufacturing industry, by means of ultrasonic non-destructive evaluation (NDE), it is very difficult to detect certain types of internal flaw using conventional instrumentation based in ultrasonic transducers located on a unique external surface of the piece under inspection. In these cases, the detection problems are due to the especial flaws orientation or their spatial location, and some technological solutions for it are still pendent to be proposed.

In addition, it is convenient, in a more general scope, to improve the flaw-location in two dimensions, by using several ultrasonic transducers emitting beams from distinct places. In fact, the utilization of more than one detection transducer provides complementary information in the NDE of many pieces. These transducers can be located at the same or at different planes depending on the piece shape and the detection necessities. In any case, the result of such arrangement is a set of ultrasonic traces, which have to be carefully fussed using digital signal processing techniques in order to extract more accurate and more complete detection results.

The usual trend for reducing the mentioned limitations in flaw detection is to increase the number of ultrasonic channels involved in the testing. On the other hand, it is important to reduce this ultrasonic channels number in order to minimize technological costs. In addition, it should be noted that the detection capability also depends on other important factors, because, from a more general point of view, still some physical limitations of the ultrasonic beams remain for a) certain angles of the scanning (Chang and Hsieh 2002), b) for certain complex geometries of the industrial components to be tested (Roy et al 1999) or c) for biological elements in medical diagnosis (Defontaine et al 2004, Reguieg et al 2006).

Schemes have been preliminarily proposed in order to improve flaw detection in difficult conditions, trying to resolve these type of aspects well with two transducers and additional digital signal processing of echoes (Chang and Hsieh 2002), or well with several arrays of few elements (Engl and Meier 2002). Other posterior alternative proposals, based on perpendicular scanning from two planes with a reduced transducers number and ultrasonic

beams overlapping, were reported (Meyer and Candy 2002, Rodríguez et al 2004). But an extensive research in order to find simple and complete solutions to these problems is still needed. In particular, the authors are currently investigating techniques for ultrasonic radiation from perpendicular planes using arrays of few radiators working in near field conditions. In parallel, we are developing digital signal processing tools for improving the signal to noise ratio (SNR) in the echoes acquired in NDE of media with complex internal structure (Lázaro et al 2002, Rodríguez et al 2004a, Pardo et al 2008).

In this technological context, a set of novel ultrasonic signal combination techniques have been developed to be applied in flaw detection ultrasonic systems based on multiple transducers. These combination techniques use a spatial-combination approach from the echographic traces acquired by several transducers located at different external planes of the piece under testing. In all these alternative techniques, the A-scan echo-information, received from the different transducers involved, is fused in a common integrated two-dimensional (2D) pattern, in which, each spot displayed incorporates distinct grades of SNR improvement, depending on particular processing parameters.

In this chapter, some linear and non-linear digital processing techniques to fuse echo-traces coming from several NDE ultrasonic transducers distributed on two perpendicular scanning planes are described. These techniques are also applied to the flaw detection by using a 2D combination of the ultrasonic traces acquired from the different transducers. The final objective is to increase the detection capabilities of unfavorable-orientation flaws and also to achieve a good 2D spatial location of them.

Individual ultrasonic echo-signals are measured by sucesively exciting several transducers located at two perpendicular planes with electrical short-time pulses. Each transducer acquires a one-dimensional (1D) trace, thus it becomes necessary to fuse all the measured 1D signals with the purpose of obtaining an useful 2D representation of the material under inspection. Three combination techniques will be presented in this chapter; they are based on different processing tools: Hilbert, Wavelets and Wigner-Vile transforms. For each case, the algorithms are presented and the mathematical expressions of the resulting 2D SNRs are deduced and evaluated by means of controlled experiments.

Simulated and experimental results show certain combinations of simple A-scans registers providing relatively high detection capacities for single flaws. These good results are obtained in spite that the very-reduced number of ultrasonic channels involved and confirm the accuracy of the theoretical expressions deduced for 2D-SNR of the combined registers.

2. Some antecedents of ultrasonic evaluation from perpendicular planes

Techniques for combining ultrasonic signal traces coming from perpendicular planes have few antecedents. As a precedent of this type of scanning performed from two distinct planes, the inspection of a high-power laser with critical optic components using ultrasonic transducers situated in perpendicular planes is mentioned in (Meyer and Candy 2002). In this particular case, the backscattering noise is valueless and the method seems centred in the combination from the arrival time of the ultrasonic echoes, and thus the combination is made with a time domain technique.

In (Rodríguez et al 2004), a testing piece containing a flaw was evaluated by using transducers located at two scanning planes. In this case, the receiving ultrasonic traces contain backscattering noise and the combination was performed in the time domain. Two combination options were there presented: one based on a 2D sum operator and the other

using a 2D product operator. The SNR was used as a quality index to evaluate both methods; and the resulting evaluation data showed a better performance of the product operator. Nevertheless, their performances were limited in both cases by the time representation of the signals.

A technique in this same line that introduces the combination in the time-frequency domain, based on the Wigner-Ville transform (WVT), was preliminary applied in (Rodríguez 2003). This technique took into account the temporal and the frequency information of the ultrasonic traces. A better SNR result than with the time domain method (Rodríguez et al 2004) was obtained. But this option presented two drawbacks: a lost of linearity of the processed signals and a high computational cost.

In (Rodríguez et al 2004b) a new method was presented, performing the combination in the time-frequency domain with a low computational cost by the use of a linear transform (based on the wavelet transform (Daubechies 1992); its 2D SNR performance seemed to be closed to that obtained in (Rodríguez 2003) with Wigner-Ville transforms.

The present chapter summarizes these three combination techniques previously proposed by the authors for flaw detection from perpendicular transducers. A comparative analysis (based on theoretic and experimental results) of their performances over a common set of specific experiments is made. The objective is to establish the respective advantages and inconveniences of each technique in a rather rigorous frame. For experimental evaluations, we have arranged an ultrasonic prototype to generate (from 2 planes) ultrasonic near-field beams collimated along the inspected piece, and to acquire the echoes from the transducers involved in our experiments. The different combination results calculated in each case, from the measured echo-responses, will be discussed.

3. Description of processing techniques for combination. Expressions of SNR

A number of distinct combination techniques to fuse several ultrasonic traces, coming from perpendicular transducers, have been proposed by the authors. There are two important parameters that define all these techniques: a) the initial type of the traces representation, and b) the particular operator utilized in their combination process.

To choose the best representation for the processing of signals is an open general problem with multiples solutions; the two most popular representations are in time or in frequency domains: a) the direct time domain is very useful for NDE problems because the spatial localization of possible defects or flaws (in the material under testing) is closely related with the apparition time of the echoes; b) the frequency domain is less used in this type of ultrasound based applications because does not permit a spatial localization; in addition, the spectrum of the ultrasonic information with interest for testing in some industrial applications, is almost coincident with the mean spectrum of the "grain" noise originated from the material texture, which some times appears corrupting the signals waveforms associated to the investigated reflectors.

An interesting possibility for introducing spectral information in these applications is the use of time-frequency representations (Cohen 1995) for the echo-graphic signals. This option shows in a 2D format the time information for the different frequency bands in which the received ultrasonic signals range. Therefore, each point of a 2D time-frequency representation corresponds with one spectral frequency and with one time instant. Two different time-frequency techniques, the wavelet transform (Daubechies 1992, Shensa 1992)

and the Wigner-Vile transform (Claasen and Mecklenbrauker 1980), will be applied in the following as complementary tools during the combination procedure.

In relation to the other abovementioned parameter defining the combination techniques, several operators to make the trace combination have been used in previous author's works: maximum, minimum, mean, median, sum and product. Theoretical and experimental results obtained by applying these operators indicate that the best performances obtained, for all the combination methods, were produced when a product operator was employed.

For this reason, we have selected (among all the possible operators) the 2D product between echo-traces, in order to properly perform the comparison among all the methods considered in this paper. In the following, the three alternative processing techniques proposed for trace combination are described, showing their performance in relation to the resultant SNR.

3.1 Time-domain combination technique

This first technique performs the combination using the envelope of the ultrasonic traces. The first step in this method is the acquisition of the traces from the ultrasonic transducers involved, which are located over two perpendicular planes in the external part of the inspected piece. The following step is the matching in time of all the different pairs of traces, each one with echo-information corresponding to precisely the same volumetric elemental area, i.e. coming from the two specific transducers which projections define such area. To reduce problems due to no perfect synchronization of the two matched traces in those pairs, the signal envelopes are utilized instead of the original signals, because this option is less sensitive to little time-matching errors. These envelopes are obtained by means of applying them the Hilbert transform. The final step is the trace combination process, by using the mentioned 2D product operator.

Briefly, the method can be resumed in four successive steps: first, the collection of the traces from the different transducers; second, the traces envelope calculation; third, the matching between the information segments of each perpendicular transducers specifically related to the same inspection area; and fourth, the combination among all the segment couples. The corresponding functional scheme is presented in Figure 1 for the particular case of four
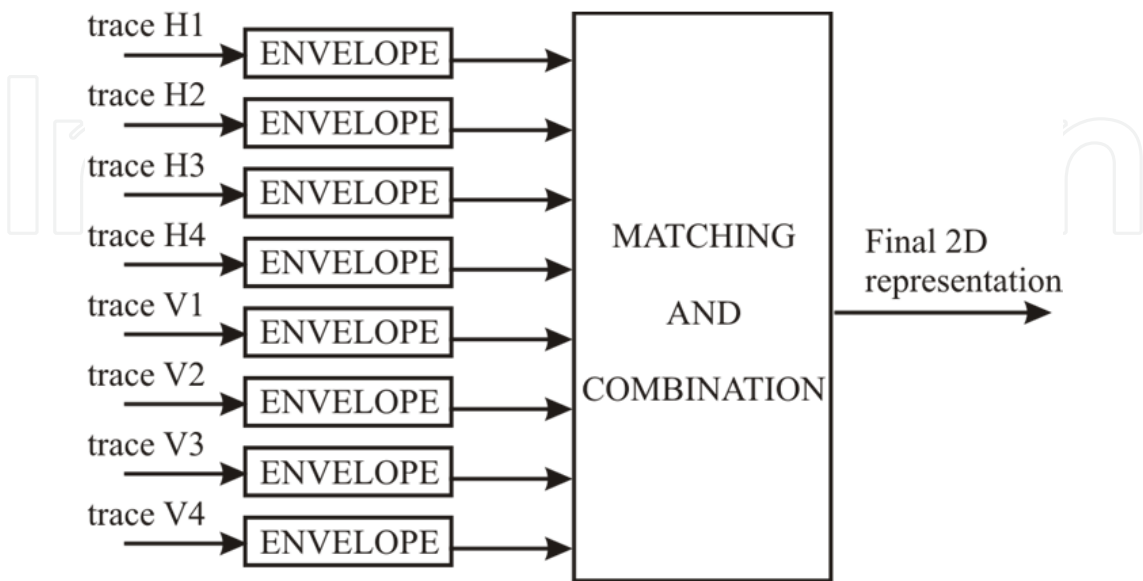

Fig. 1. Functional scheme of the time-domain echo-traces combination technique.

ultrasonic transducers (H1, H2, H3 and H4) with horizontal propagation beams and four
transducers (V1, V2, V3 and V4) with vertical propagation beams.

Some theoretical characterizations of this method, including statistical distributions of the
combined noise and some results about SRN enhancements were presented in (Rodríguez et
al 2004). The more important result of that work is the expression of the resulting SNR for
the 2D ultrasonic representation after the combination process.

The SNR of the initial traces, SNR_{ini}, containing an echo-pulse and noise, is defined as:

$$SNR_{ini}(dB) = 10\log\frac{\frac{1}{M}\sum_{i=1}^{M}(p(i))^2}{\frac{1}{L}\sum_{i=1}^{L}(n(i))^2} \tag{1}$$

where, p denotes the echo-pulse and n represents the noise; M is the length of the pulse and
L is the length of the whole ultrasonic trace.

The SNR of the final 2D representation is:

$$SNR_{2D}(dB) = 10\log\frac{\frac{1}{M^2}\sum_{i=1}^{M}\sum_{j=1}^{M}(p_{2D}(i,j))^2}{\frac{1}{L^2}\sum_{i=1}^{L}\sum_{j=1}^{L}(n_{2D}(i,j))^2} \tag{2}$$

where, p_{2D} and n_{2D} denotes the 2D representation of the echo-pulse and of the grain noise; M
and L are the dimensions of the 2D rectangular representations of the echo-pulse and of the
ultrasonic trace, respectively.

The SRN of the 2D representation obtained by using this time-domain combination method,
SNR_{2Dtime}, can be expressed as a function of SNR_{ini} :

$$SNR_{2Dtime}(dB) = 2 \cdot SNR_{ini}(dB) \tag{3}$$

In consequence, the resulting SNR with this method, SNR_{2Dtime} , expressed in dB, is the
double of the initial SNR of the A-scans before combination (SNR_{ini}).

3.2 Linear time-frequency combination technique

The time-domain traces combination, previously described, works without any frequency
consideration. In order to obtain a further improving of SNR, it would be necessary to use
some type of processing in the frequency domain. Nevertheless, the ultrasonic echoes
coming from flaws in some NDE applications, and the grain noise produced by the own
material structure, have similar global mean spectra, which difficult the flaw discrimination
in the frequency domain. But if these spectra are instantaneously analyzed, it can be
observed that the instantaneous spectrum is more regular for echo-signal than for grain
noise. The tools that permit the analysis of these differences between signal and noise are
the time-frequency representations, which can be obtained by using a linear or also a non-
linear transformation.

In this section, we will deal with the application of linear time-frequency representations to
improve our signal-combination purpose. The two most popular linear time-frequency

representations are the Short-Time Fourier Transform and the Wavelet transform (Hlawatsch and Boudreaux-Barlets 1992). Both types of transforms can be implemented in an easy way by means of linear filter banks.

In the present linear technique, the combination process begins with the time-frequency representation of the all the acquired ultrasonic traces. A linear time-frequency transform is applied and the frequency bands with maximum ultrasonic energy are selected in each trace. The number of selected bands will be denoted as L. At this point, we have to resolve L problems similar to that presented in the previous time-domain combination method. In this way, L separate 2D displays are produced, one for each frequency band. The final step is the combination of these 2D displays by using a point-to-point product of them. A simple case, where combination is performed by selecting the same frequency bands for all the transducers, was presented in (Rodríguez et al 2004b), but also it could be possible to make the combination by using different bands for each transducer. The method scheme is presented in the Figure 2 for 4 horizontal and 4 vertical transducers.

Here, the combination for each frequency band is similar to the case of the time-domain technique. Then, it will be necessary to make the following steps: a) to match in time the common information of the different transducer pairs (for each frequency band), b) to calculate the time-envelope for all the bands selected in each trace, c) to perform the combinations obtaining several one-band 2D representations, and d) to fuse all these 2D displays, so resulting the final 2D representation.
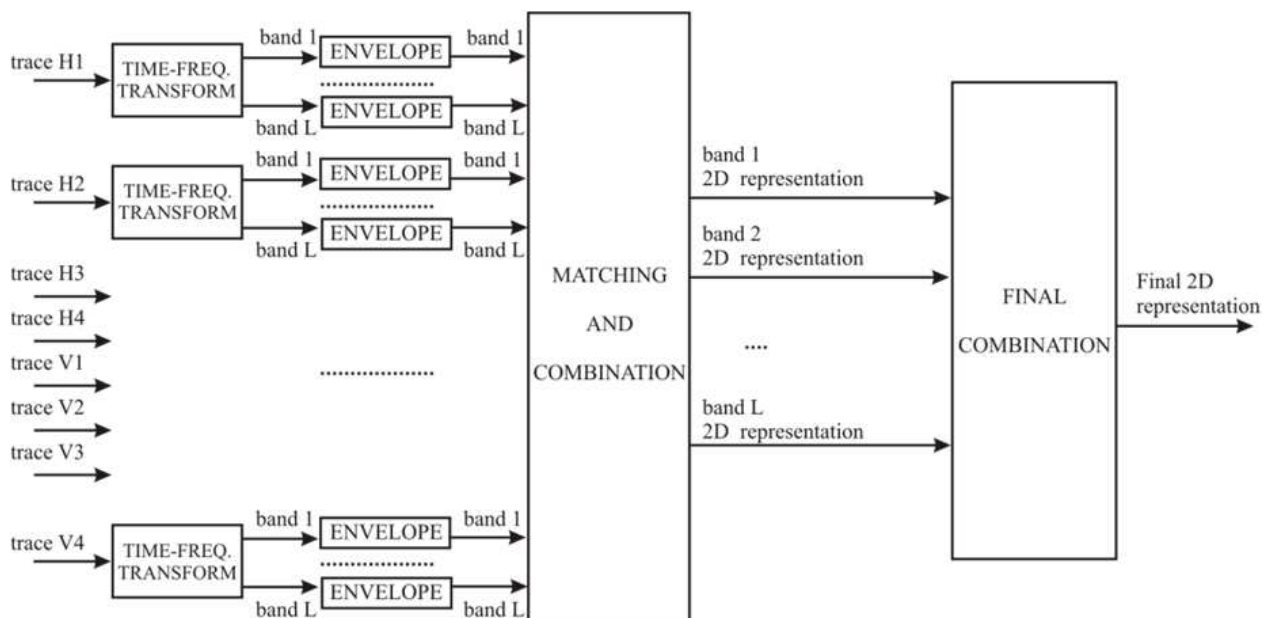

Fig. 2. Functional scheme of the linear time-frequency traces combination technique

The matching process can be common for all the frequency bands if the point number of the initial traces is maintained and if the delays of the filtering process are compensated in each band. The SNR of the 2D representation of each individual band, $SNR_{2DTFlinear}^{(band-i)}$ is obtained from expression (3).

$$SNR_{2DTFlinear}^{(band-i)}(dB) = 2 \cdot SNR_{ini}(dB) \tag{4}$$

The final global SNR, after the combination of all the 2D displays belonging to the different frequency bands, $SNR_{2DTFlinear}$, can be obtained supposing that the 2D representations for each band are independent and perfectly synchronized (Rodríguez et al 2004b):

$$SNR_{2DTFlinear}(dB) = 2 \cdot L \cdot SNR_{ini} \quad (dB) \qquad (5)$$

being, L, the number of the selected frequency bands.

Consequently, in this case, the resulting $SNR_{2DTFlinear}$ presents an important factor of improvement over the SNR_{ini}. This factor is the double of the number of frequency bands used in the combination. It must be noted that comparing expressions (5) and (3), the SNR improvements is multiplied by L, but the computational complexity of the algorithm is also multiplied by the same factor L. In the experimental results section of this chapter, the accuracy of this expression will be confirmed comparing (5) with simulations using as linear time-frequency tool the undecimated wavelet packet transform (Shensa 1992, Coifman and Wickerhauser 1992). In any case, it must be noted that this expression is also valid for any linear time-frequency transform.

3.3 Wigner-Ville Transform (WVT) combination technique

The non-linear time-frequency distributions present some advantages over linear transforms, but some non-linear terms ("cross-terms") appear degrading the quality of the distributions and usually the computational cost is incremented. One of the most popular non-linear time-frequency representations is the Wigner-Ville transform (WVT) (Claasen and Mecklenbrauker 1980), which has been previously utilized in ultrasonic applications with good results (Chen and Guey 1992, Malik and Saniie 1996, Rodríguez et al 2004a).

The WVT presents an useful property for dealing with ultrasonic traces: its positivity for some kind of signals (Cohen 1995). In order to illustrate the suitability of this transform for the processing of the ultrasonic pulses typical in NDE applications, we will show that they fulfil that property. For it, an ultrasonic pulse-echo like to those acquired in such NDE equipment can be approximately modelled by the following expression:

$$p(t) = A \cdot e^{-(at^2/2)} \cos(\omega_0 t) \qquad (6)$$

where A is the pulse amplitude, a is a constant related to the duration and bandwidth of the pulse ($a>0$), and ω_0 is the central frequency of its spectrum.

The WVT of the ultrasonic pulse modelled by (6) is (Rodríguez 2003):

$$WVT_P(t,\omega) = \frac{A^2}{(a\pi)^{\frac{1}{2}}} \cdot e^{-(at^2/2)-(\omega-\omega_0)^2/a} \qquad (7)$$

The expression (7) shows that the WVT of an ultrasonic pulse with Gaussian envelope has only positive values. The chirp with Gaussian envelope is the most general signal for which the WVT is positive through-out the time-frequency plane (Cohen 1995). The ultrasonic grain noise does not carry out this property, so resulting that the sign of the WVT values represents a useful option to discriminate this type of difficult-to-eliminate noise of the echo pulses coming from real flaws.

The combination method begins in this case by calculating the WVT in all the ultrasonic traces. After the band selection is performed, the negative values (that correspond mainly

with noise) are set to cero. For each frequency band, a combination is made by using the 2D product operator, like as it was used in the time-domain combination technique. The final 2D representation is obtained with a point to point product of all the 2D displays related to the different frequency bands. A functional scheme of this WVT based combination method is presented in the Figure 3, for the case of eight transducers considered in this section.
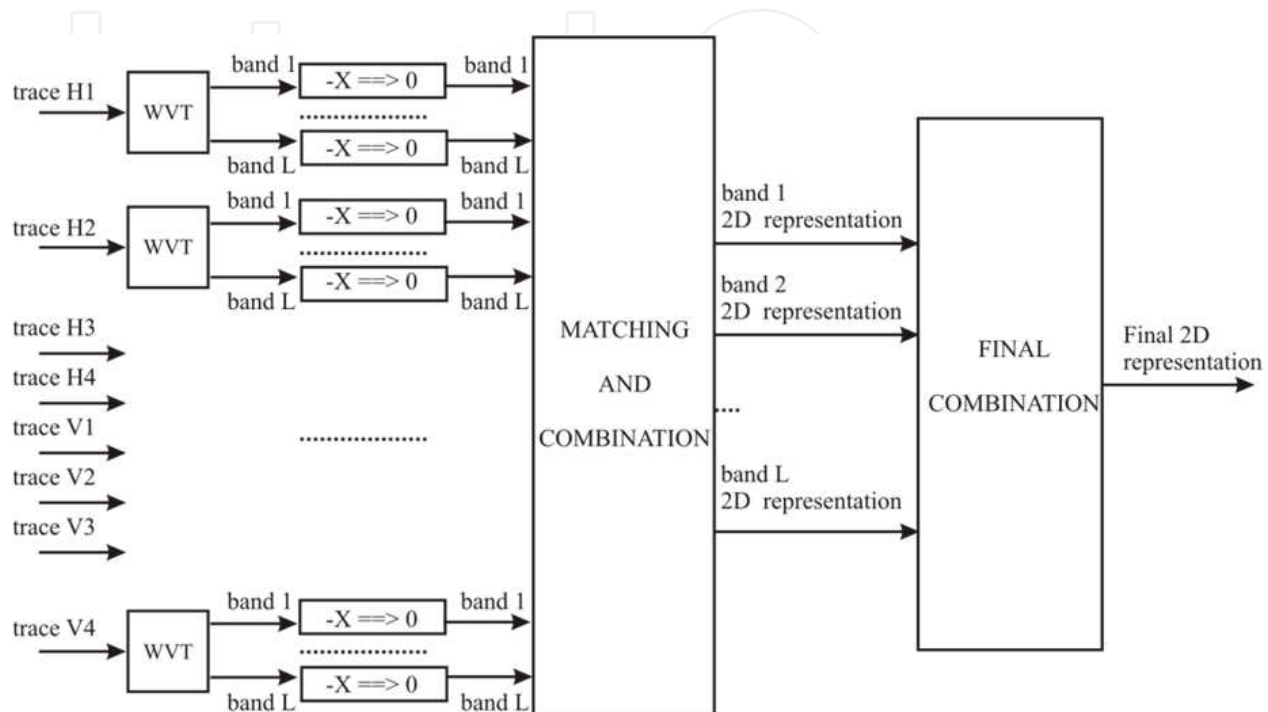

Fig. 3. Functional scheme of the WVT traces combination method.

A good estimation of the resulting SNR for the 2D representation in this WVT case, SNR_{2DWVT}, can be obtained from the results presented in (Rodríguez 2003):

$$SNR_{2DWVT}(dB) \cong 3 \cdot L \cdot SNR_{ini} \quad (dB) \tag{8}$$

Therefore, the improvement factor of the SNR, expressed in dB, which can be obtained by this WVT method, is the triple of the number of frequency bands that had been selected.

In consequence, the theoretic improvement levels in the SNR provided by the three alternative techniques for combining ultrasonic traces coming from two perpendicular transducers, (i.e., the basic option using traces envelope product, and the others two options based on linear time-frequency and WVT trace decompositions), are quite different.

So, the quality of the resulting 2D combinations, in a SNR sense, is predicted to be quite better when time-frequency decompositions are chosen, and the best results must be expected for the Wigner-Ville option, which in general seems to be potentially the more effective processing. Nevertheless, in spite of these good estimated results for the WVT case, it must be noted that in general this option supposes higher computational cost. Therefore, the more effective practical option should be decided in each NDE situation depending on the particular requirements and limitations in performance and cost being needed. In the following sections, the confirmation of these predictions will be carried out, by means of several experiments from simulated and measured ultrasonic traces.

4. Protocols used in the different testing experiments

Two types of experiments (I and II) have been designed with the purpose of evaluating and comparing the three trace combination methods presented in the previous section. The comparison will be performed over the same set of ultrasonic traces for the three cases. The type-I experiments are based on simulated noisy ultrasonic traces and those of type-II use experimentally acquired echo-traces. The protocols used in these experiments are an extension of those we have planned in references (Rodríguez et al 2004a, Rodríguez 2003, Rodríguez et al 2004b).

4.1 Experiments type-I based on simulated noisy traces

Type-I experiments were carried out with simulated signal registers. They provide adequate calculation results to confirm the accuracy of the expressions estimated from the theoretical models of the processing techniques proposed in the equations (3), (5) and (8) to predict the distinct SNRs (SNR_{2Dtime}, $SNR_{2DTFlinear}$ and SNR_{2DWVT}). So, those expressions could be validated for an ample range of values in SNR_{ini} with perfectly controlled characteristics in echo-signals and their associated grain noises. Some results, in a similar context, using these same rather simple simulated registers, have been compared in a previous work (Rodríguez et al 2004a) with the obtained results when a more accurate ultrasonic trace generator was used. A very close agreement between them was observed, which confirms the suitability of these registers to evaluate those expressions.

The testing case proposed to attain this objective is the location of a punctual reflector into a rectangular parallelepiped from 2 external surfaces, perpendicular between them, and using 4 transducers by surface. The general scheme of these experiments, with 4 horizontal (H1, H2, H3, H4) and 4 vertical (V1, V2, V3, V4) transducers is depicted in the Figure 4. Transducers H3 and V2 receive echoes from the reflector whereas the other transducers (H1, H2, H4, V1, V3 and V4) only receive grain noise. To assure compatibility of experiments type-I with experiments type-II, ultrasonic propagation in a piece of 24x24 mm has been simulated assuming for calculations a propagation velocity 2670 m/s very close to that corresponding to methacrylate material. The sampling frequency was 128 MHz.
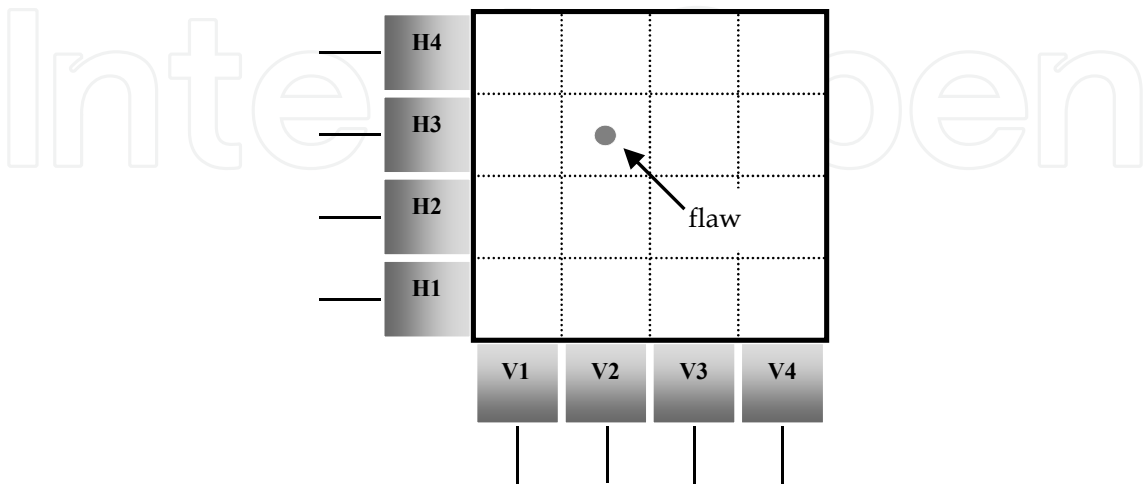

Fig. 4. Geometry of the inspection case planned to evaluate the different combination methods: detection of a single-flaw in a 2D arrangement with 16 elemental-cells.

The simulation of the echo-traces produced by the reflector was made by integrating a real echographic signal with a synthetic noise-component similar to the grain reflections registered in some industrial inspections, and that are quite difficult to be cleaned. The echographic echo was acquired from one of the 4 MHz transducers of the perpendicular array used for experiments type-II. The sampling frequency was 128 MHz. The echo is shown in figure 5. The "coherent" grain noise, to be associated with the basic echo-signal, was obtained by means of a synthetic white gaussian noise generator. To assure the frequency coherence with the main reflector echo-pulse (simulating an unfavourable case), this initial noise register was passed thought a digital filter just having a frequency response as the ultrasonic echo-pulse spectrum. Finally, the composed traces containing noisy echoes are obtained by the addition of the real echo-signals with the synthetic noise register. Previously, the noise had been unit power normalized and the echo-signal had been multiplied by a constant with the finality of obtaining the desired SNR_{ini}.
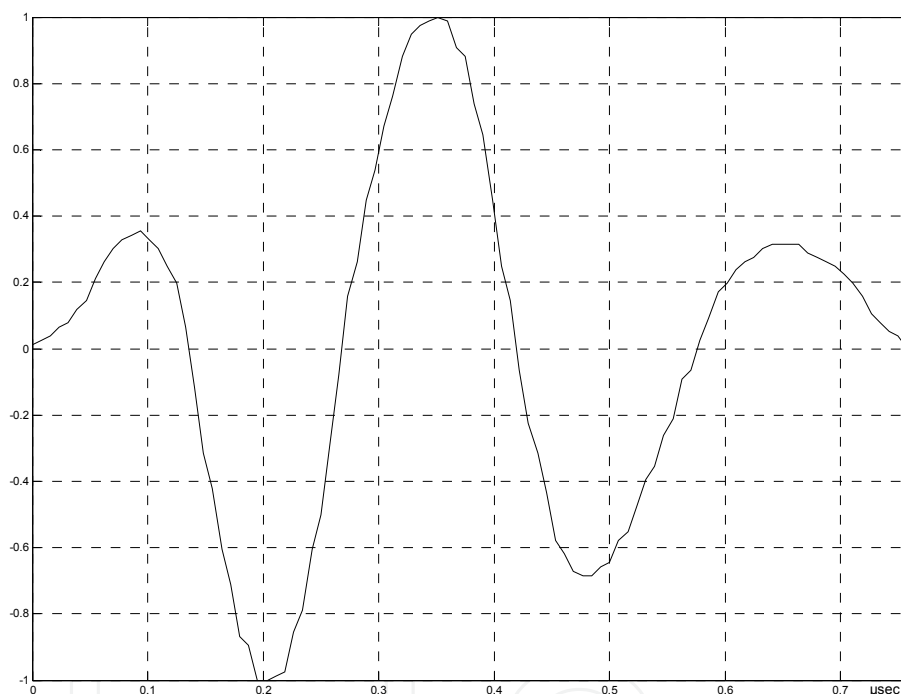

Fig. 5. Ultrasonic echo utilised in type-I experiments.

Several sets of tests were prepared with 11 different SNR_{ini} (0, 1, 2, 3, 4, 5, 6, 7, 8, 9 and 10 dB). For each SNR_{ini}, 10.000 tests were performed using the three combination methods described in section 3, and their respective results were compared. The length of the each individual ultrasonic trace was of 2304 points (corresponding to 18 microseconds with a sampling frequency of 128 MHz). 18 microseconds is the time of flight of 48 (24 +24) mm with a propagation velocity of 2670 m/s, very close to the total echo length from the methacrylate piece considered in experiments. The length of the echo-signals contained in these traces was of 98 samples. The size of the final 2D representation is 2304x2304 (5308416) points (corresponding with an inspected area of 24x24 mm). Thus, from 18432 initial points (2304 by transducer), a 2D display with 5308416 points was obtained for the whole piece. To measure the different SNR's, the echo-signal power was measured over its associated area 98x98 points in the 2D display, whereas for the noise power, the rest of the 2D display points were used.

4.2 Experiments type-II with echographic traces measured from an ultrasonic prototype

The type-II experiments are based on real ultrasonic echoes measured from an isolated-flaw (hole drilled in a plastic piece) with a multi-channel ultrasonic prototype designed for this kind of tests in laboratory. The two array transducers are disposed in a perpendicular angle and the square plastic piece with the hole are inside and in contact with the radiation area of arrays. There are 4 broadband elemental transducers in each perpendicular array, 8 in the whole system. Transducers work in the 4 MHz frequency band range. The dimensions of the emitting surface of each individual transducer are 6x6 mm, being 24 mm the total length of both arrays. Then, the area of the methacrylate piece to be inspected by the ultrasonic system is 24x24 mm. Arrays manufacturing was ordered to the Krautkramer company. The methacrylate piece has a drilled cylindrical hole in a position similar as used in experiment type I. Then, simulations of experiment type-I are almost coincident with real measurements of experiment type-II. The main difference is that methacrylate generates a very low level of ultrasonic grain noise. Figure 6 shows the disposition of transducers and inspected piece.
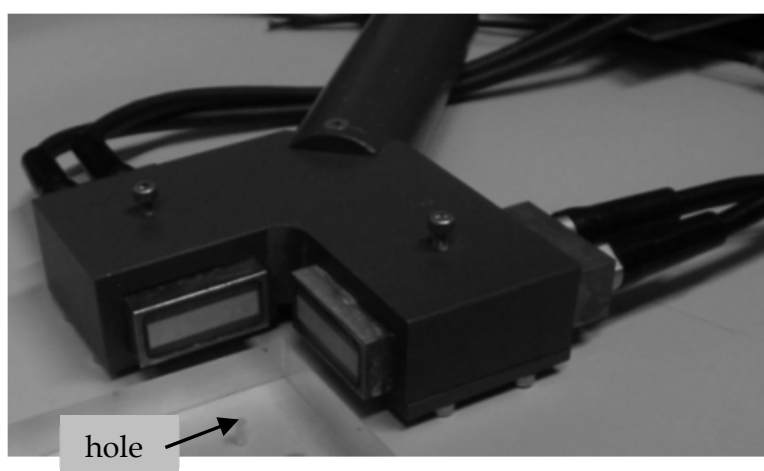

Fig. 6. Perpendicular array transducers and the inspected plastic piece with the hole.

In all the measurement cases, the transducers are driven for transmission and selected for echoe reception in a sequential way. We deal with near field radiations and only one transducer emits and receives at the same time, in our eight-shots successive measurement process. Thus, among all the echoes produced by the isolated reflector in each transducer shot, only those received in the two transducers located in front of the reflector (at the perpendicular projections of the flaw on the horizontal and vertical apertures) will be captured, because, in each shot, the echoes acquisitions are cancelled in the other seven transducers. Additionally, these two transducers in front of the reflector could receive certain amount of noise. And under these conditions, the rest of transducers of the two array apertures, in each plane, only could eventually acquire some noise signal during its shot, but not echoes from the reflector hole. Concretely, in the flaw scheme of the figure 4 (before shown for the simulated type-I experiments), the pulsed-echoes from the discontinuity of the reflector will be received by transducers H3 and V2 (with the apparition time of these echoes being determined by the distance to each transducer and the sound propagation velocity in the piece), and the traces in H1, H2, H4, V1, V3 and V4, will not contain flaw reflections.

For measurements, an experimental prototype, with eight ultrasonic transceivers, has been arranged for the validation and comparative assessment of the three flaw localization techniques by 2D traces combination in a real NDE context. It includes as emitter-receiver probes two 4 MHz piezoelectric linear arrays of 4 elements each one (as it is shown in figure 6), which are controlled by a Krautkramer NDE system model USPC-2100, disposed in the pulse-echo mode. The main characteristics of this NDE system in the signal receiving stage are the following: a dynamic range of 110 dB; a maximum effective sampling of 200 MHz in the digitalizing section. A signal gain of 44 dB and a sampling rate of 128 MHz were selected in reception for all the signal acquisitions performed in this work. Other general characteristics of this system are: pulse repetition rate of up to 10 KHz per channel, and 15 MHz of effective bandwidth in emission-reception. The high-voltage pulser sections of this commercial system were programmed in order to work with the highest electric excitation disposable for the driven transducers, which is about 400 Volts (measured across a nominal load of 100 Ohm). A relatively low value for the E/R damping resistance of 75 Ohm was selected looking for the assurance of a favourable SNR and a good bandwidth in the received echoes. Finally, the maximum value offered by this equipment for the energy level, contained into the driving spike, was selected.

It must be noted that in the experimental ultrasonic evaluations performed with the two arrays, their elemental transducers were operated with the restriction of that only one transducer was emitting and receiving at the same time. So, the two transducers located in front of the flaw (in this case: transducers H3 & V2) were operated separately as receivers in order to obtain useful information from the artificially created flaw (by drilling the plastic piece), which is clearly smaller than transducer apertures. Thus, only ultrasonic beams of H3 & V2 transducers (which remain collimated into a 6 mm width due to the imposed near-field conditions) attain the hole, whereas the other six elemental transducers radiate theirs beams far away of that hole, and therefore, in any case, they are not covering the artificial flaw and are not receiving echoes reflected from this flaw during their acquisition turns.

5. Simulated and experimental flaw detection results for the three combination techniques. Discussion of their performance

Three sets of experiments are shown in this section. First, the results related to the final SNR calculated for seven type-I simulated experiments using different combination options will be presented in the first section part. Second, 2D displays about the location of an isolated reflector, calculated for a particular combination case and a small SNR_{ini} are also shown. Third, as results illustrating the type-II experiments, 3 pairs of representations of a real flaw obtained by means of the 3 different combination techniques of section 3 will be shown and commented, analyzing the respective performances of the three techniques. The initial data for these type-II experiments were a set of measured ultrasonic traces acquired with the ultrasonic set-up of section 4.

The first tasks in type-I experiments (with simulated traces) were performed to confirm the accuracy of expressions (3), (5) and (8). In these experiments, 11 SNR_{ini} were selected (0, 1, 2, 3, 4, 5, 6, 7, 8, 9, 10). 10.000 sets of measures were generated using a real 4 MHz echo response sampled at 128 MHz and synthetic noise, composed in this case by 66.66% of white Gaussian noise (accounting by the "thermic" noise induced by the usual

electronic instrumentation) and 33.34% of coherent noise (accounting by "grain" noise tied to material texture). Seven experiments were realized: 1 with time domain technique, 3 based on linear time-frequency decomposition using 2, 3 and 4 bands, and finally 3 utilising WVT with 2, 3 and 4 band again. The SNR after the 7 experiments were measured. The results are exposed in Tables 1 and 2, together with the values expected from expressions (3), (5) and (8).

In the first column of Tables 1 and 2, the initial SNR, SNR_{ini} of the ultrasonic traces are shown. The experiment 1 in the Table 1 was planned in order to measure the behaviour of the 2D time-combination method in terms of SNR_{2Dtime} improvement. The experiments number 2, 3 and 4 had as objective to evaluate the accuracy of the expression $SNR_{2DTFlinear}$ corresponding with the linear time-frequency combination. The difference among these 3 cases is the number of bands utilized [parameter L in expression (5)]; thus, the experiments 2, 3 and 4 were performed with 2, 3 and 4 bands respectively. The particular linear time-frequency transform used in these latter experiments was the undecimated wavelet packet transform, (Mallat 1989, Shensa 1992, Coifman and Wickerhauser 1992), with Daubechies 4 as mother wavelet, as it was used in the work (Rodríguez et al 2004b) but with some new adjusts included in this case, which provide a better agreement (as it can be seen in Table 1) between estimated and measured expressions of $SNR_{2DTFlinear}$ that in the mentioned work.

Finally, experiments 5 to 7 in Table 2 show the improvements obtained by using the WVT transform in the combination. The differences among these 3 WVT experiments are again the number of bands being involved: 2, 3 or 4, respectively. The SNR related to these 7 experiments are presented in Table 1 and Table 2. The expected SNRs estimated from their theoretic expressions, together with the measured SNRs, are detailed for each case. The measured SNR values, which are shown in these tables, were calculated as the mean of different 10.000 SNRs obtained for each set of simulated traces.

SNR$_{ini}$ (dB)	SNR$_{2Dtime}$(dB) experiment 1		SNR$_{2DTFlinear}$(dB)					
			2 bands experiment 2		3 bands experiment 3		4 bands experiment 4	
	Est.	Meas.	Est.	Meas.	Est.	Meas.	Est.	Meas.
0	0	0.11	0	0.34	0	0.05	0	0.75
1	2	2.08	4	3.53	6	5.72	8	8.81
2	4	4.07	8	7.62	12	11.54	16	16.63
3	6	6.06	12	11.46	18	17.53	24	24.57
4	8	8.11	16	15.42	24	23.41	32	32.26
5	10	9.97	20	19.39	30	29.34	40	40.44
6	12	12.01	24	23.43	36	35.28	48	48.42
7	14	14.11	28	27.38	42	41.23	56	56.24
8	16	16.13	32	31.34	48	47.31	64	64.25
9	18	18.16	36	35.32	54	53.24	72	72.17
10	20	20.08	40	39.33	60	59.27	80	80.43

Table 1. SNRs of the 2D representations obtained by means of the experiments 1 to 4.

SNR_{ini} (dB)	SNR_{2DWVT}(dB)					
	2 bands experiment 5		3 bands experiment 6		4 bands experiment 7	
	Est.	Meas.	Est.	Meas.	Est.	Meas.
0	0	4.93	0	8.64	0	12.88
1	6	8.90	9	12.81	12	18.08
2	12	11.91	18	19.01	24	25.31
3	18	16.76	27	28.02	36	38.92
4	24	21.63	36	35.70	48	50.45
5	30	27.65	45	45.32	60	64.33
6	36	34.63	54	56.13	72	80.90
7	42	41.53	63	63.17	84	94.67
8	48	48.91	72	78.46	96	111.31
9	54	56.88	81	90.69	108	127.91
10	60	64.24	90	101.73	120	142.04

Table 2. SNRs of the 2D representations obtained by means of the experiments 5 to 7.

The estimated and measured values of the SNR_{2Dtime} (Table 1, columns 2 and 3) and $SNR_{2DTFlinear}$ ratios, obtained for 2 bands (Table 1, columns 4 and 5), 3 bands (Table 1, columns 6 and 7) and 4 bands (Table 1, columns 8 and 9), present a very good agreement. Finally, the SNR_{2DWVT} (Table 2) for different bands number show a high correlation between estimated and measured values, but in some cases small differences appear. These are due to the fact that the estimated expression for SNR_{2DWVT} was obtained by means of approximations, but in any case, the global correspondence between estimated and measured values is also reasonably good.

Apart from SNR improvements, the three techniques described in this chapter allow the accurate detection of flaws inside pieces.

A second type-I experiment was realised to show this good accuracy in the defect detection capability inside the pieces. A new set of ultrasonic traces was generated, simulating again a hole in a rectangular piece as it is depicted in figure 4. In this case, the selected SNR_{ini} of the initial A-scan was 3 dB.

The echo is the real 4 MHz trace sampled at 128 MHz, and the noise contained in the initial eight traces was composed by white noise and coherent noise with amplitudes of 50% each one. This set of simulated measures is displayed in figure 7, being the units shown in horizontal axis micro-seconds. In these graphics, it can be appreciated that noise and echo amplitudes are similar, thus it is very difficult to distinguish the reflector echo from the noise. In fact, the echo only appears in graphics corresponding to transducers H3 and V2. The real echo-pulse of H3 transducer is located in the middle of the noise beginning approximately at 5.5 microseconds whereas the echo-pulse of V2 transducer begins around 10.75 microseconds.

Using the ultrasonic registers of figure 7, the three combinations of the traces by applying the different techniques exposed in the chapter were performed. The first combination was done using the time domain method and the resulting 2D representation is shown in figure 8.a., where the 24x24 mm inspected area is displayed (the axis units are in mm). The searched hole location is around 8 mm in horizontal axis and 15 mm in vertical axis. It can
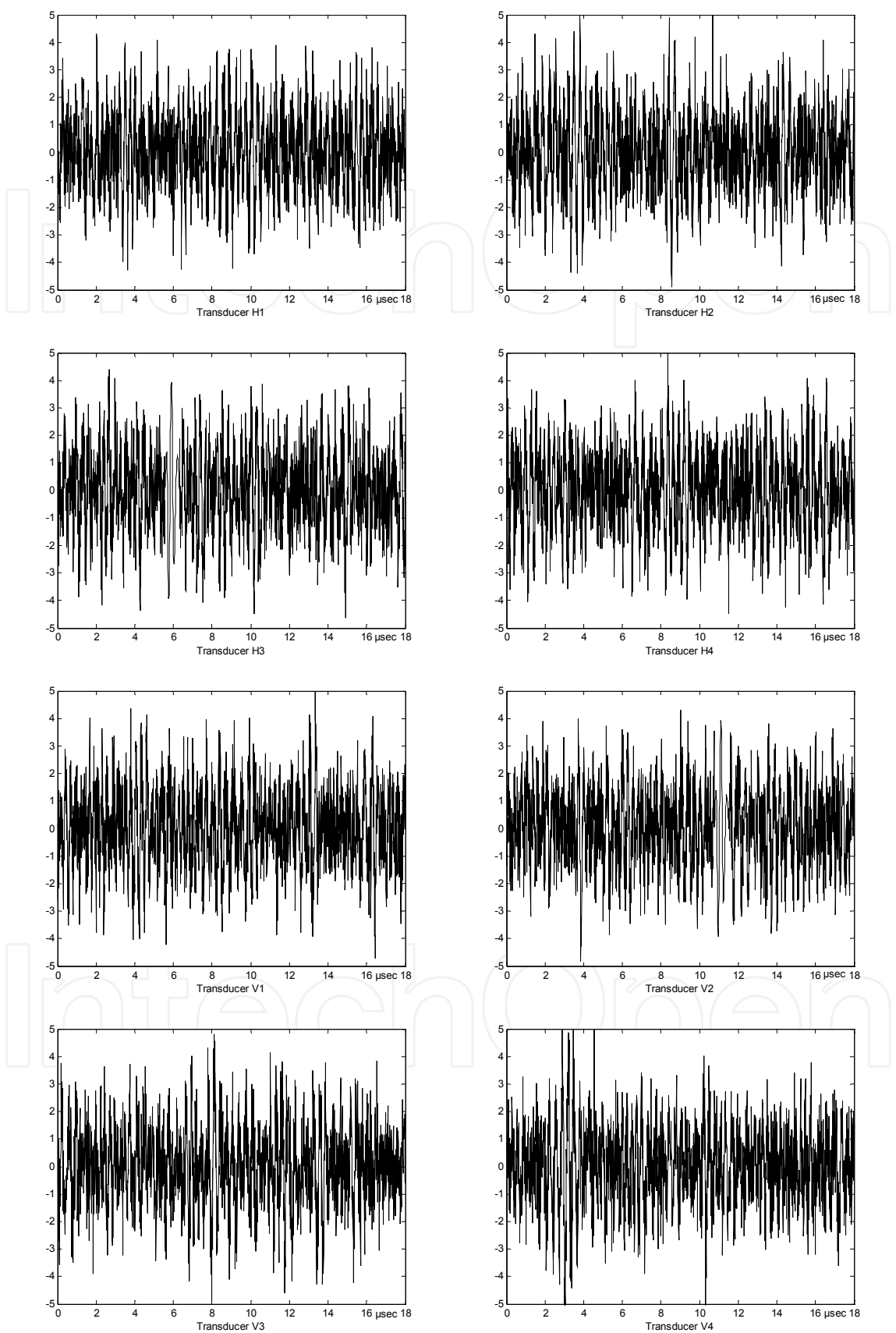
Fig. 7. Ultrasonic traces from the 8 transducers of figure 4 with a simulated SNR_{ini} = 3 dB.

be deduced that by using this time domain technique, the flaw is not very well marked and a lot of noise appear, but it is must taken into account that, in the initial traces shown in figure 7, the echo level was under noise level, in some cases.

The linear time-frequency transform used for second combination in this comparative analysis was the undecimated wavelet packet transform with Daubechies 4 as mother wavelet, as in the previous set of experiments. Figures 8.b, 8.d and 8.e show the 2D representations obtained using wavelets with 2, 3 and 4 bands. In these graphics, which amplitudes are in linear scale, it can be clearly distinguished the mark corresponding to the hole. Figure 8.f represents the same result than 8.e, but with the gray scale of amplitudes measured in dB, in order to appreciate with more detail the low levels of noise.

Finally figures 8.c, 8.g and 8.h show the 2D representations obtained using WVT with 2, 3 and 4 bands and using a linear scale for amplitudes. Figure 8.h and 8.i correspond to the same results, but figure 8.i is displayed with its amplitude scale expressed in dB. Thus, in figure 8.h, the noise has disappeared but in figure 8.i the low level noise can still be observed. It must be noted that, for all the cases, the 2D representations of figure 8 mark the flaw that we are looking for, although in the initial traces, shown in figure 7, the echoes coming from the flaw were very difficult to see.

Additionally, in the first strip of the figure 8, the 2D graphic resulting when time domain method is used, is shown. It can be seen its performance in contrast with the wavelet method with minimum quality (L=2) and WVT option with minimum quality (L=2), in such a way that a quick comparison can be made among improvements applying the different methods.

In that concerning to results of type-II experiments, displays of 2D representations, obtained by combination of experimental traces acquired from the ultrasonic prototype described in section 4 are presented in figure 9. Two scales have been used for each 2D result: linear and logarithmic scales. With the logarithmic scale, the small flaw distortions and secondary detection indications, produced by each combination method, can be more easily observed and quantified. It must be noted that the logarithmic scales have an ample resolution of 60 dB, giving a better indication of techniques performance.

In all these cases, the initial traces had a low level of grain noise because these echo-signals correspond to reflections from the small cylindrical hole drilled in a plastic piece made of a rather homogeneous material without internal grains. The patterns of figure 9 were obtained using similar processing parameters than those used with the simulated traces in the type-I experiments, and only two bands were considered for frequency decomposition. The results of the figure 9, using the time-combination method, present clear flaw distortions (more clearly visible in 9.b) with shadow zones in form of a cross, but even in this unfavourable case, a good spatial flaw location is achieved.

The mentioned crossing distortions appear already very attenuated in the results shown in figures 9.c and 9.d, corresponding to the linear time-frequency combination technique (wavelet using 2 bands), and practically disappear in the results of figures 9.e and 9.f obtained by using to the WVT combination technique.

Similar good results could be also achieved in many practical NDE cases with isolated-flaws patterns, but this performance could be not extended to other more complicated testing situations whit flaws very close among them, i.e. with two or more flaws located into a same elemental cell and thus being insonifyed by the same two perpendicular beams. Under these more severe conditions, some ambiguity situations, with apparition of "phantom" flaws, could be produced [Rodríguez et al 2005]. We are working order to propose the extension of

this type of ultrasonic traces combination methods (using perpendicular NDE transducers) from echoes coming from two ultrasonic imaging array apertures, where this particular restriction (for only isolated reflectors) will be solved, by means of an improved procedure, that includes an additional processing step involving additional echographic information acquired not only from the emitting transducers.
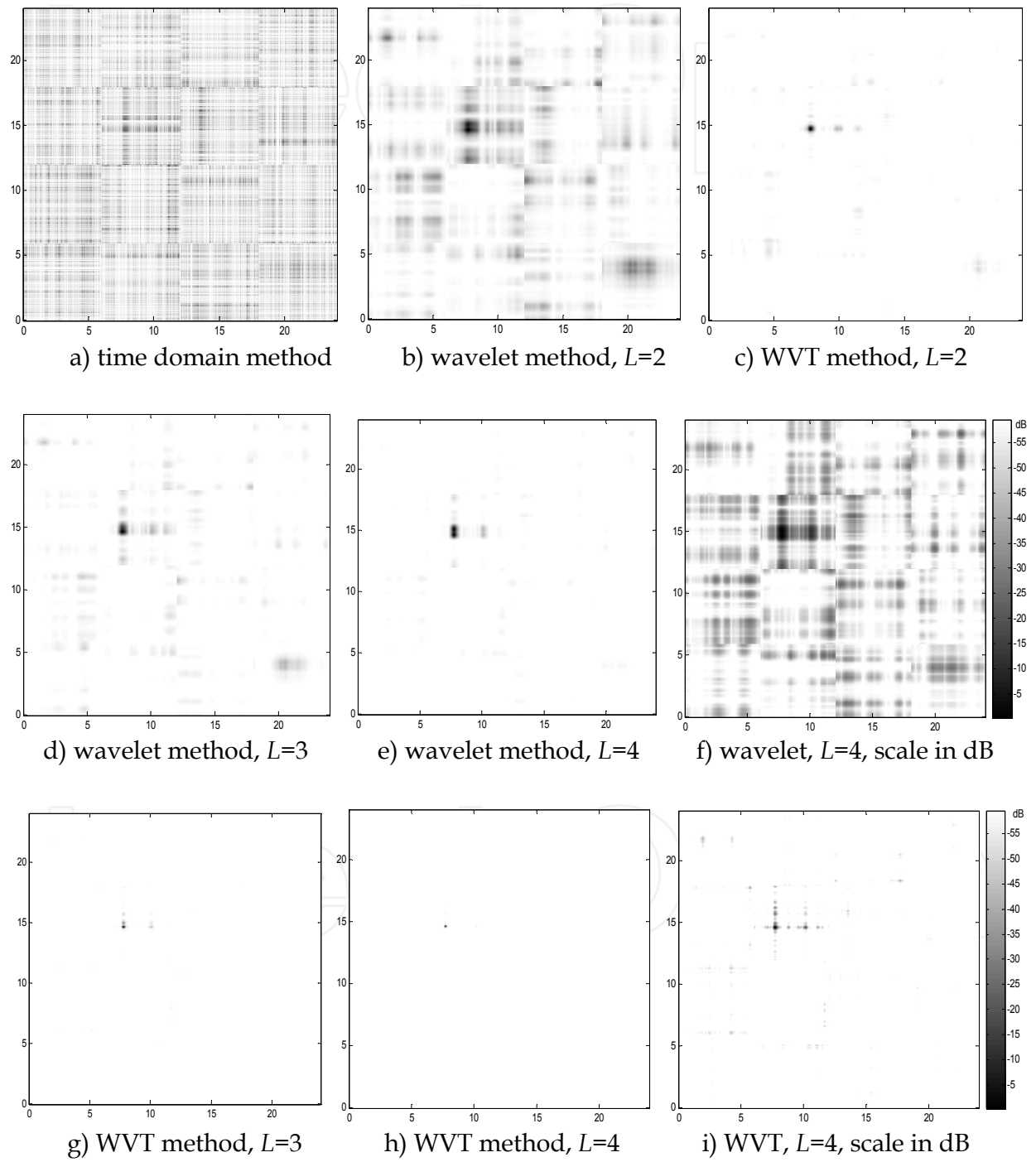

Fig. 8. Different 2D representations, after the combination of the traces shown in the figure 7; different methods and *L* values were used.

6. Conclusion

Three variants of a recent digital signal processing procedure for ultrasonic NDE, based on the scanning with a small number of transducers sized to work in near field conditions (located at two perpendicular planes to obtain different ultrasonic perspectives), are evaluated. They originate distinct techniques to fuse echo information coming from two planes: time-domain, linear time-frequency, and WVT based, 2D combination methods.
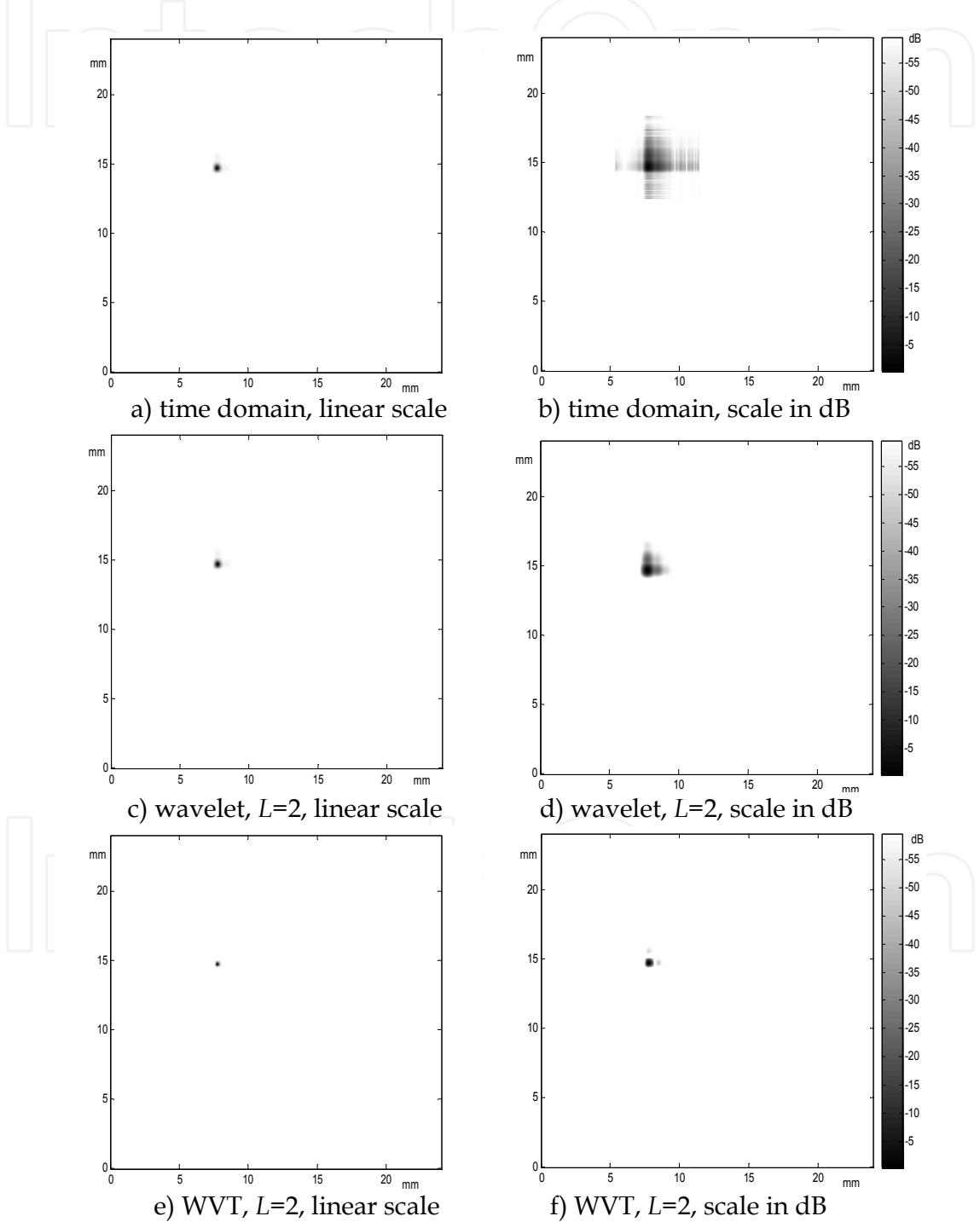

a) time domain, linear scale

b) time domain, scale in dB

c) wavelet, *L*=2, linear scale

d) wavelet, *L*=2, scale in dB

e) WVT, *L*=2, linear scale

f) WVT, *L*=2, scale in dB

Fig. 9. Different 2D representations after combination of real traces in experiments type-II, with linear scale (a, c, e) and logarithmic scale (b, d, f).

Two types of experiments have been performed to evaluate these techniques. Results of the first type, involving simulated noisy signal traces, have confirmed the accuracy of our theoretical SNR expressions proposed for the three combination variants. The first type experiments also demonstrate a great capability for accuracy detection of internal flaws.

Results from the second type, using an experimental ultrasonic prototype, permit to validate the proposed methods in a real NDE context.

More concretely, the three combination methods described and applied in this chapter, based on different processing tools (the Hilbert, Wigner-Ville, and Undecimated Wavelet packet Transforms) produce accurate 2D displays for isolated-flaws location. Additionally, these methods drastically improve the SNR of these 2D displays in relation to the initially acquired traces, very especially with the two latter processing cases, being the best flaw discrimination results obtained with the WVT option, but with a mayor computational cost than the wavelet technique, which also offers a good performance.

These good results for isolated-flaws patterns could be not directly extended to other more complicated testing situations with flaws very close among them, because some ambiguous flaw indications could be produced. In a future work, this particular restriction will be addressed by means of a specifically extended imaging procedure.
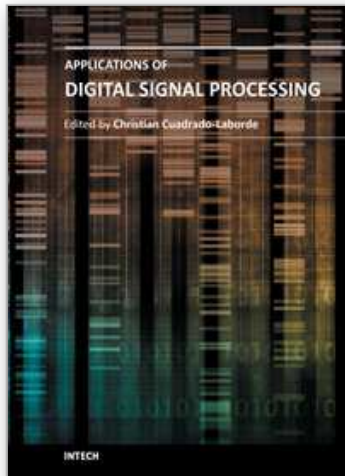
7. Acknowledgment

8. References

Chang Y F and Hsieh C I 2002 Time of flight diffraction imaging for double-probe technique *IEEE Trans. Ultrason. Ferroel, Freq. Cont.* vol 49(6), pp 776-783.

Chen C.H. and Guey J.C. 1992 On the use of Wigner distribution in Ultrasonic NDE *Rev. of Progress in Quantitative Nondestructive Evaluation*, vol. 11A, pp. 967-974,.

Claasen T.A.C.M. and Mecklenbrauker W.F.G. 1980 The Wigner Distribution - A tool for time-frequency signal analysis *Philips J. Res.*, vol. 35, pp. 217-250, 276-300, 372-389.

Cohen L 1995 *Time-Frequency Analysis* Prentice Hall PTR Englewood Cliffs New Jersey.

Coifman R. and Wickerhauser M.V. 1992 Entropy-based algorithms for best basis selection *IEEE Trans. on Information Theory*, vol. 38, pp. 713-718.

Daubechies I 1992 *Ten Lectures on Wavelets* Society for Industrial and Applied Mathematics PhiladelphiaPA

Defontaine M, Bonneau S, Padilla F, Gomez M.A, Nasser Eddin M, Laugier P and Patat F 2004 2D array device for calcaneus bone transmission: an alternative technological solution using crossed beam forming *Ultrasonics* vol 42, pp 745-752.

Engl G and Meier R 2002 Testing large aerospace CFRP components by ultrasonic multichannel conventional and phased array pulse-echo techniques *NDT.net* vol. 7 (10).

Hlawatsch F and Boudreaux-Barlets G 1992 Linear and Quadratic Time-Frequency Signal Representations *IEEE Signal Processing Magazine* vol 9(2), pp. 21-67.

Lazaro J C, San Emeterio J L, Ramos A and Fernandez-Marron J L 2002 Influence of thresholding procedures in ultrasonic grain noise reduction using wavelets *Ultrasonics* vol. 40, pp 263-267.

Malik M.A.and Saniie J. 1996 Performance comparison of time-frequency distributions for ultrasonic non-destructive testing *Proc .IEEE Ultrasonic Symposium*, pp. 701-704.

Mallat S 1989 A theory for multiresolution signal decomposition: the wavelet representation *IEEE Transaction on Pattern Analysis and Machine Intelligence* vol 11, pp 674-693.

Meyer A W and Candy J V 2002 Iterative Processing of Ultrasonic Measurements to Characterize Flaws in Critical Optical Components *IEEE Trans. on Ultrason. Ferroel. and Freq. Cont.* vol 8, pp 1124-1138.

Pardo E, San Emeterio J L, Rodríguez M A and Ramos A 2008 Shift Invariant Wavelet Denoising of Ultrasonic Traces *Acta Acustica United with Acustica* vol 94 (5), pp 685-693.

Reguieg D, Padilla F, Defontaine M, Patat F and Laugier P 2006 Ultrasonic transmission device based on crossed beam forming *Proc. of the 2006 IEEE Ultrasonic Symposium*, pp. 2108-2111

Roy O, Mahaut S and Serre M 1999 Application of ultrasonic beam modeling to phased array testing of complex geometry components. *Review of Progress in Quantitative Non destructive Evaluation* Kluwer Acad. Plenum Publ. NewYork vol 18, pp. 2017-2024.

Rodríguez M A 2003 Ultrasonic non-destructive evaluation with spatial combination of Wigner-Ville transforms *ndt&e international* vol 36 pp. 441-445.

Rodríguez M A, Ramos A and San Emeterio J L 2004 Localization of isolated flaws by combination of noised signals detected from perpendicular transducers *NDT&E International* 37, pp. 345-352.

Rodríguez M A, San Emeterio J L, Lázaro J C and Ramos A 2004a Ultrasonic Flaw Detection in NDE of Highly Scattering Materials using Wavelet and Wigner-Ville Transform Processing *Ultrasonics* vol 42, pp 847-851.

Rodríguez M A, Ramos A, San Emeterio J L and Pérez J J 2004b Flaw location from perpendicular NDE transducers using the Wavelet packet transform *Proc. IEEE International Ultrasonics Symposium 2004* (*IEEE Catalog 05CH37716C*), pp 2318-2232.

Rodríguez M A, Ramos A and San Emeterio J L 2005 Multiple flaws location by means of NDE ultrasonic arrays placed at perpendicular planes *Proc. IEEE International Ultrasonics Symposium 2005* (*IEEE Catalog 0-7803-9383-X/05*), pp. 2074-2077.

Shensa M, 1992, The discrete wavelet transform: wedding the trous and Mallat algorithms, *IEEE Trans. Signal Process*, vol. 40, pp. 2464-2482.

Applications of Digital Signal Processing

Edited by Dr. Christian Cuadrado-Laborde

In this book the reader will find a collection of chapters authored/co-authored by a large number of experts around the world, covering the broad field of digital signal processing. This book intends to provide highlights of the current research in the digital signal processing area, showing the recent advances in this field. This work is mainly destined to researchers in the digital signal processing and related areas but it is also accessible to anyone with a scientific background desiring to have an up-to-date overview of this domain. Each chapter is self-contained and can be read independently of the others. These nineteenth chapters present methodological advances and recent applications of digital signal processing in various domains as communications, filtering, medicine, astronomy, and image processing.

How to reference

In order to correctly reference this scholarly work, feel free to copy and paste the following:

Miguel A. Rodrîguez-Hernández, Antonio Ramos and J. L. San Emeterio (2011). Comparative Analysis of Three Digital Signal Processing Techniques for 2D Combination of Echographic Traces Obtained from Ultrasonic Transducers Located at Perpendicular Planes, Applications of Digital Signal Processing, Dr. Christian Cuadrado-Laborde (Ed.), ISBN: 978-953-307-406-1, InTech, Available from: http://www.intechopen.com/books/applications-of-digital-signal-processing/comparative-analysis-of-three-digital-signal-processing-techniques-for-2d-combination-of-echographic

INTECH
open science | open minds